Human Molecular Genetics, 2013, Vol. 22, No. 11 **2141–2151**
doi:10.1093/hmg/ddt067
Advance Access published on February 14, 2013

The cytochrome *b* p.278Y>C mutation causative of a multisystem disorder enhances superoxide production and alters supramolecular interactions of respiratory chain complexes

Anna Ghelli[1], Concetta V. Tropeano[1], Maria Antonietta Calvaruso[1], Alessandra Marchesini[1], Luisa Iommarini[1], Anna Maria Porcelli[1], Claudia Zanna[1], Vera De Nardo[2], Andrea Martinuzzi[2], Flemming Wibrand[3], John Vissing[4], Ivana Kurelac[5], Giuseppe Gasparre[5], Nur Selamoglu[6], Fevzi Daldal[6,*] and Michela Rugolo[1]

[1]Dipartimento di Farmacia e Biotecnologie, Università di Bologna, Via Irnerio 42, Bologna 40126, Italy, [2]Istituto Scientifico 'E. Medea', Conegliano Veneto 31015, Italy, [3]Department of Clinical Genetics, Rigshospitalet, University of Copenhagen, Copenhagen, Denmark, [4]Neuromuscular Clinic and Research Unit, Department of Neurology, Rigshospitalet, University of Copenhagen, Copenhagen, Denmark, [5]Dipartimento di Scienze Mediche e Chirurgiche, Unità di Genetica Medica, Università di Bologna, Bologna 40138, Italy and [6]Department of Biology, University of Pennsylvania, Philadelphia, PA 19104, USA

Received October 30, 2012; Revised and Accepted February 8, 2013

Cytochrome *b* is the only mtDNA-encoded subunit of the mitochondrial complex III (CIII), the functional bottleneck of the respiratory chain. Previously, the human cytochrome *b* missense mutation m.15579A>G, which substitutes the Tyr 278 with Cys (p.278Y>C), was identified in a patient with severe exercise intolerance and multisystem manifestations. In this study, we characterized the biochemical properties of cybrids carrying this mutation and report that the homoplasmic p.278Y>C mutation caused a dramatic reduction in the CIII activity and in CIII-driven mitochondrial ATP synthesis. However, the CI, CI + CIII and CII + CIII activities and the rate of ATP synthesis driven by the CI or CII substrate were only partially reduced or unaffected. Consistent with these findings, mutated cybrids maintained the mitochondrial membrane potential in the presence of oligomycin, indicating that it originated from the respiratory electron transport chain. The p.278Y>C mutation enhanced superoxide production, as indicated by direct measurements in mitochondria and by the imbalance of glutathione homeostasis in intact cybrids. Remarkably, although the assembly of CI or CIII was not affected, the examination of respiratory supercomplexes revealed that the amounts of CIII dimer and III_2IV_1 were reduced, whereas those of $I_1III_2IV_n$ slightly increased. We therefore suggest that the deleterious effects of p.278Y>C mutation on cytochrome *b* are palliated when CIII is assembled into the supercomplexes $I_1III_2IV_n$, in contrast to when it is found alone. These findings underline the importance of supramolecular interactions between complexes for maintaining a basal respiratory chain activity and shed light to the molecular basis of disease manifestations associated with this mutation.

INTRODUCTION

Ubiquinol:cytochrome *c* oxidoreductase [cytochrome bc_1 or respiratory complex III (CIII), EC 1.10.2.2] is the central complex of the respiratory chain. In mammalians, it comprises 11 subunits among which cytochrome *b* is the only one encoded by the mitochondrial genome. Together with the iron/sulfur (Fe/S) protein and cytochrome c_1 subunits,

*To whom correspondence should be addressed. Tel: +1 2158984394; Fax: +1 2158988780; Email: fdaldal@sas.upenn.edu

© *The Author 2013. Published by Oxford University Press. All rights reserved.*
For Permissions, please email: journals.permissions@oup.com

cytochrome *b* forms the catalytic core of CIII. Cytochrome bc_1 oxidizes reduced quinone (QH_2) via an unstable semi-quinone intermediate at a catalytically active site (Q_o). Through a sophisticated mechanism with two 'one-electron' transfer steps, one to a high potential chain (involving the Fe/S protein and cytochrome c_1) and another to a low potential chain (comprising the hemes b_L and b_H of cytochrome *b*), CIII contributes to the generation of the proton motive force ($\Delta\mu H^+$) across the membrane with minimal energy expenditure (1,2). In its native form, CIII is dimeric and is closely associated in varying proportions with CI and CIV to form supramolecular structures, referred to as supercomplexes or 'respirasomes' (3). The occurrence of such supercomplexes as structural entities has been documented recently (3–5) and the ability to respire has also been revealed, confirming their functional role (6). However, the physiological implications of such specific supramolecular interactions are not yet fully understood. It has been proposed that the formation of supercomplexes could provide significant kinetic advantages by enhancing electron flow by direct channeling of substrates and products (oxidized and reduced ubiquinones) as well as by reducing the amounts of undesired reactive oxygen species (ROS) overproduction (7). A consistent body of evidence, accumulated in recent years, has demonstrated that supercomplexes have a central role in the etiology and pathogenesis of different mitochondrial diseases. In particular, the finding of combined CI–CIII defects in a subset of patients with a genetic defect in CIII strongly suggested a tight interaction between these two respiratory enzymes (8,9). Conversely, mutation of the nuclear-encoded CI gene *NDUFS4* also resulted in a reduction in the CIII activity in addition to CI deficiency (10). Indeed, it has been demonstrated very recently that in the absence of NDUFS4, CIII stabilizes CI (11). Altogether, these findings point out to a structural relationship between CIII and CI and are consistent with the existence in the respiratory chain of supercomplex(es) in which cytochrome *b* plays a key role. However, most mutations that affect CIII, including cytochrome *b*, do not impair CI activity. CIII function is normal in most mutations located in genes encoding CI subunits (12), indicating that the specific alteration(s) induced by different mutation(s) depends on the specific amino acid positions in the affected protein.

Mutations in cytochrome *b*, including deletions, frameshifts, termination and missense mutations, are among the least common abnormalities identified to date in humans (12). Nevertheless, they exhibit a large spectrum of mitochondrial disease symptoms ranging from pure muscle symptoms, mostly exercise intolerance (13), to multisystem disorders (14–16).

Recently, studies on the bacterial enzyme have proposed that specific amino acids at the Q_o site of cytochrome bc_1 might provide protective mechanisms against oxidative damage. Namely, a conserved Tyr residue at position 302 of *Rhodobacter capsulatus* cytochrome *b* is critical for this process, and its substitution with other amino acids decreases CIII activity and concomitantly enhances superoxide production (17). Remarkably, the Tyr302 to Cys substitution leads to chemical cross-linking of cytochrome *b* to the Fe/S subunits, rendering the bacterial enzyme inactive and sensitive to the oxidative disintegration of its catalytic [2Fe/2S] cluster (17). Interestingly, the same mutation at this conserved residue at position 278 of human cytochrome *b* (p.278Y>C, m.15579A>G) has also been encountered in a patient with severe exercise intolerance and a multisystem disorder (deafness, retinitis pigmentosa, cataract, cognitive impairment, growth retardation and epilepsy) (16). These observations prompted us to exploit the findings obtained in the bacterial model to shed light on the pathogenic mechanisms underlying the human disease associated with the same cytochrome *b* mutation (17). The results presented in this work strongly suggest that the deleterious effects of cytochrome *b* p.278Y>C mutation are mitigated when CIII is assembled into the supercomplexes $I_1III_2IV_n$, underlining the importance of supramolecular interactions between respiratory complexes on disease manifestations associated with this mutation and possibly with significant general implications on the onset of mitochondrial diseases.

RESULTS

Transfer of the mutant mtDNA in the cybrid cells confirms the pathogenicity of the m.15579A>G mutation

The first step of our study was to generate cybrid clones from the patient fibroblast cell line carrying the m.15579A>G heteroplasmic mutation (16), with the aim to obtain the most suitable unbiased cell model to work with. Several syngeneic clones were obtained, differing only at nucleotide 15579, as confirmed by complete sequencing, and showing various degrees of the mutation load, initially evaluated by polymerase chain reaction (PCR)/restriction fragment length polymorphism (data not shown). Putative wild-type, homoplasmic and heteroplasmic mutant clones were selected and the presence of the mutation was confirmed by Sanger sequencing (Supplementary Material, Fig. S1). The mutant load of the heteroplasmic clones was then evaluated by denaturing high-performance liquid chromatography (DHPLC; Supplementary Material, Fig. S2), which allows quantification with sensitivity of 2% (18). Figure 1A and Supplementary Material, Figures S1 and S2 show that one of these clones (cl.5) was 100% wild-type, three were heteroplasmic, exhibiting 58% (cl. 4), 78% (cl. 3) and 96% (cl. 2) mutation loads, and one clone (cl.1) was the homoplasmic mutant (100% mutant mtDNA). To estimate the effect of the different mutation load on the mitochondrial energetic function, we investigated the viability of these cybrid clones during incubation in a glucose-free medium containing galactose and pyruvate [Dulbecco's modified Eagle medium (DMEM)-galactose]. Under these conditions, the rate of glycolysis is markedly reduced, and cells are forced to rely solely on oxidative phosphorylation for ATP production (19). Figure 1B shows that after 16–24 h incubation in DMEM-galactose, the viability of the homoplasmic mutated clone was dramatically decreased compared with control cybrids. Conversely, clones bearing 58, 78 and 96% mutation loads were not significantly different from wild-type cybrids, with almost 60% of cells still viable after 48 h in DMEM-galactose. As described in a previous study (20), the reduced viability of the wild-type clone is likely due to the nutrient shortage in the growth medium that was not refreshed during the incubation time.

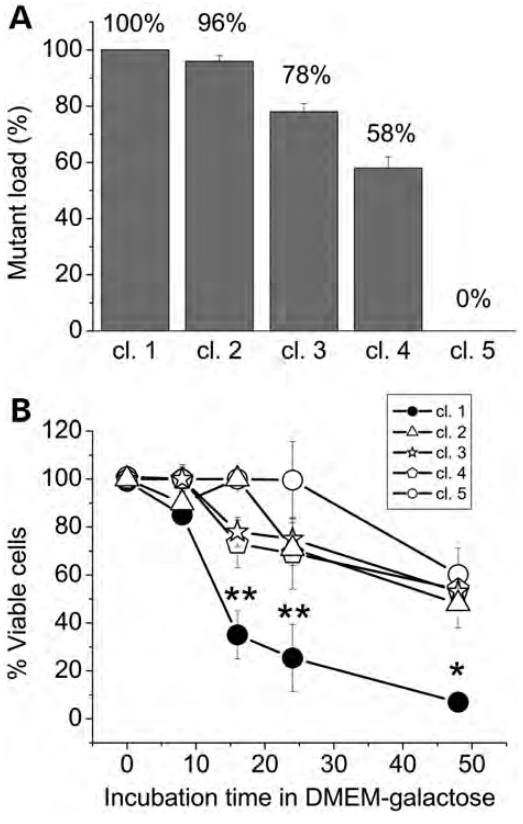

Figure 1. The load of m.15579A>G mutation and viability in the galactose medium of cybrid clones. (**A**) The homo-/heteroplasmic state of the cybrid clones as evaluated by the Sanger sequencing and DHPLC analysis. (**B**) Cybrid clones were incubated in DMEM-galactose for the times indicated. The m.15579A>G (p.278Y>C) mutation load of each clone is indicated in parenthesis. The SRB absorbance value at time zero corresponds to 100% viable cells. Each data point represents the mean ± SEM of at least four determinations. Asterisk denotes the values statistically different from wild-type ($^{*}P < 0.05$; $^{**}P < 0.01$).

These results are in agreement with previous reports showing that the threshold for defective respiration and growth in the galactose medium was very high, close to 90% in cybrids bearing a frame-shift mutation inducing a cytochrome *b* gene deletion (21). Our subsequent studies were then performed in the control cell line (referred to as wild-type) and in the homoplasmic 100% mutant clone (from now on referred to as Y278C) to dissect the biochemical effects of this mutation avoiding any interference due to the presence of small quantities of wild-type mDNA.

The p.278Y>C mutation affects dramatically both CIII activity and CIII-driven ATP synthesis, but does not compromise the overall mitochondrial energetic function

The measurement of CI [reduced form of nicotinamide adenin dinucleotide (NADH):decyl-benzoquinone (DB):2, 6-dichloroindophenol (DCIP) oxidoreductase], CIII (DBH_2: cytochrome *c* oxidoreductase), CI + CIII (NADH:cytochrome *c* oxidoreductase) and CII + CIII (succinate:cytochrome *c* oxidoreductase) activities were determined in crude mitochondria (22,23). In cells bearing the p.278Y>C mutation, the CIII activity was almost completely lost (~ 95% lower), whereas the CI + CIII activity was less affected (65% lower) when compared with controls (Fig. 2A). Previously, a similar quasi-complete loss of CIII activity was also observed with the *R. capsulatus* enzyme carrying the homologous cytochrome *b* mutation (p.302Y>C) (17). It is noteworthy that the activities of CI and CII + CIII were not significantly different in the two cell lines (Fig. 2A). It seems therefore that the p.278Y>C mutation affects the CIII but not the CI activity. Further analysis of the oxidative phosphorylation function was performed by measuring the rate of mitochondrial ATP synthesis. ATP synthesis of digitonin-permeabilized p.278Y>C cybrids was significantly decreased (~ 35%) in the presence of CI substrates (malate/pyruvate), and this decrease was even more pronounced
(~ 85%) in the presence of the CIII substrate (DBH_2) compared with control cybrids. However, only a slight not significant reduction was observed in the presence of the CII substrate succinate (Fig. 2B). To further evaluate the energetic competence of mutant cybrids, mitochondrial membrane potential ($\Delta\psi_m$) was measured by the accumulation of the fluorescent cationic probe tetramethylrhodamine (TMRM) after addition of oligomycin, a specific inhibitor of F_1F_O ATPase. Accumulation of TMRM was not affected by oligomycin in both control and mutated cells (Fig. 2C and D), whereas the subsequent addition of the CIII inhibitor antimycin A caused a rapid release of the probe (i.e. mitochondrial depolarization). Noticeably, a slower depolarization was observed in both cell lines after the addition of the CI inhibitor rotenone, indicating that $\Delta\psi_m$ was sustained by a contribution of electron flow through CII or other quinone reductases. Given that the TMRM distribution only provides a qualitative measurement of $\Delta\psi_m$, we believe that the subtle difference in the rate of rotenone-induced TMRM release between control and mutated cybrids (shown in Fig. 2C and D) was not significant. Taken together, these results clearly indicated that the cytochrome *b* p.Y278C mutation causes a severe impairment of CIII activity in cybrids, leading to decreased oxidative phosphorylation efficiency, but does not affect $\Delta\psi_m$ driven by the electron transport through the respiratory chain.

The p.278Y>C mutation enhances superoxide production and perturbs glutathione homeostasis

Recently, it has been demonstrated that the *R. capsulatus* cytochrome *b* p.302Y>C substitution, which is homologous to human cytochrome *b* p.278Y>C, induced ROS production by CIII and cross-linking between cytochrome *b* and Fe/S subunits by a disulfide bond (17). To evaluate whether the human mutation also promoted ROS production, the rate of superoxide generation by crude mitochondria isolated from control and mutated cybrids was determined using the same enzymatic assay as described previously (17). As shown in Figure 3A, the mutated CIII produced detectable (~10%) amounts of ROS measured as manganese-superoxide dismutase (SOD)-sensitive and stigmatellin-sensitive (i.e. CIII-specific) cytochrome *c* reductase activities.

Since the role of glutathione in the detoxification of a number of oxidizing species, including ROS derived from mitochondria, has been extensively demonstrated (24), we

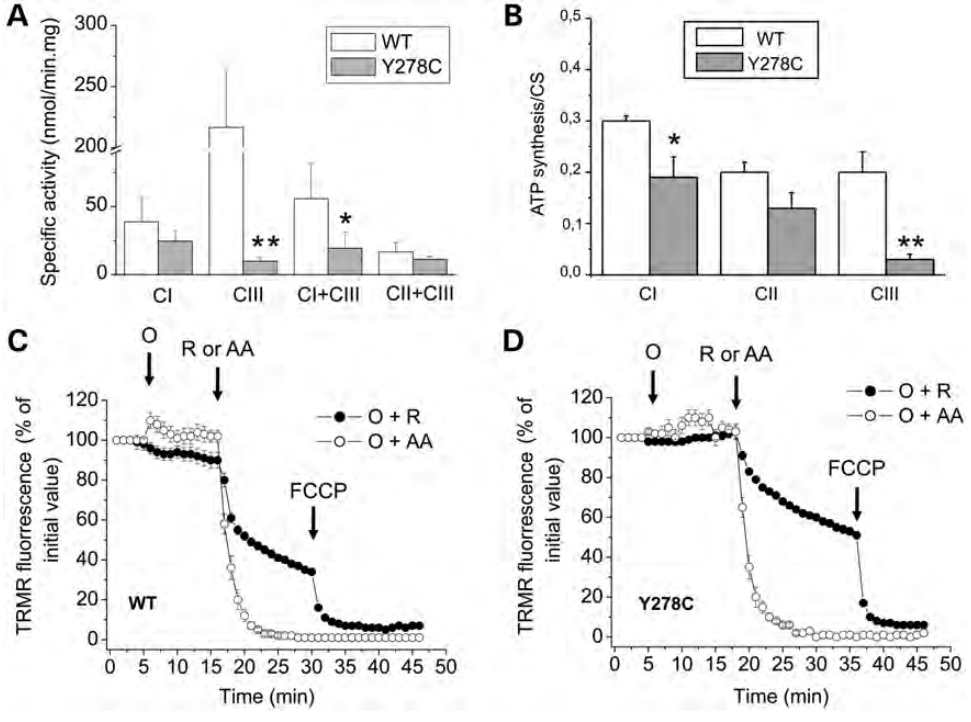

Figure 2. Mitochondrial energetic function. (**A**) Respiratory complexes activities: CI (NADH:DB:DCIP), CIII (DBH_2:cytochrome *c*), CI + CIII (NADH:cytochrome *c*) and CII + CIII (succinate:cytochrome *c*) activities were determined in crude mitochondria, isolated as described in Materials and Methods. Data are presented as the means ± SD of at least six determinations. Asterisk denotes the values significantly different from controls ($^{*}P < .05$; $^{**}P < 0.01$). (**B**) ATP synthesis: digitonin-permeabilized cybrids were incubated with 5 mM malate plus 5 mM pyruvate (CI) or 10 mM succinate plus 4 μM rotenone (CII) or 50 μM DBH_2 (CIII), and the rate of the mitochondrial ATP synthesis was measured as described in Materials and Methods. Data were normalized for the CS activity, which was similar in both clones. Data are presented as the means ± SD of at least four determinations. Asterisk denotes the values statistically different from controls ($^{*}P < 0.05$; $^{**}P < 0.01$). (**C** and **D**) Mitochondrial membrane potential: cybrids were loaded with TMRM as described in Materials and Methods. Where indicated, 4 μM rotenone (R), 3 μM antimycin A (AA), 6 μM oligomycin (O) and 4 μM FCCP were added. Data are presented as the means ± SD of 3–5 determinations.

also determined the amounts of reduced glutathione (GSH) and oxidized glutathione (GSSG) in cybrids grown in glucose- or galactose-containing media. Although the GSSG/GSH + GSSG ratio was only slightly increased in DMEM-grown mutant cybrids in comparison with wild-type cells (data not shown), a significant increase was detected after 6 h of incubation in DMEM-galactose (Fig. 3B), a time point where most of the mutant cells were still viable (Fig. 1B). This finding indicated that an imbalance in the homeostasis of this major intracellular antioxidant, possibly as a consequence of the superoxide production by the mutated CIII, becomes apparent when cells are forced to use oxidative metabolism and precedes death. This result prompted us to determine whether the addition of exogenous antioxidants might ameliorate the viability of mutated cells incubated in the galactose medium. As illustrated in Figure 3C, addition of the selective superoxide scavenger sodium 4,5-dihydroxybenzene-1, 3-disulfonate (Tiron; 10 mM) improved the viability of mutated cybrids after 24 h incubation in DMEM-galactose (48% increase). Furthermore, the presence of 10 mM GSH or *N*-acetylcysteine (NAC) significantly increased the viability already after 16 h of incubation (30 and 76% increase, respectively) and also after 24 h of incubation (54 and 32% increase, respectively). All these compounds slightly reduced the viability of control cybrids. Taken together, these results indicate that the loss of viability of cybrids carrying the cytochrome *b* p.278Y>C mutation in DMEM-galactose is due, at least in part, to an imbalance of the GSSG/GSH ratio as a consequence of increased superoxide production. Finally, the CI, CIII and CI + CIII activities were assessed in crude mitochondria isolated in a buffer containing dithiothreitol (DTT), which reduces the thiol groups. Accordingly, CIII and CI + CIII activities increased significantly in mutant mitochondria, but not in control (Fig. 3D and E). These results suggested that the human cytochrome *b* p.278Y>C mutation enhanced superoxide production by CIII in cybrids, and likewise, enzymatic activities of the respiratory complexes were better preserved under reducing conditions to significantly improve cell viability.

The p.278Y>C mutation has no effect on the assembly of CI and CIII

We then inquired whether the p.278Y>C mutation alters the steady-state expression level of respiratory complex subunits and the assembly of CIII and/or CI. Mitoplasts lysates were analyzed by sodium dodecyl sulfate–polyacrylamide gel electrophoresis (SDS–PAGE) followed by immunoblot. As shown in Figure 4A, the levels of representative subunits of different complexes were similar in control and mutant cybrids when their ratios to porin present in each case were compared. Similarly, semi-quantitative analyses of the fully assembled

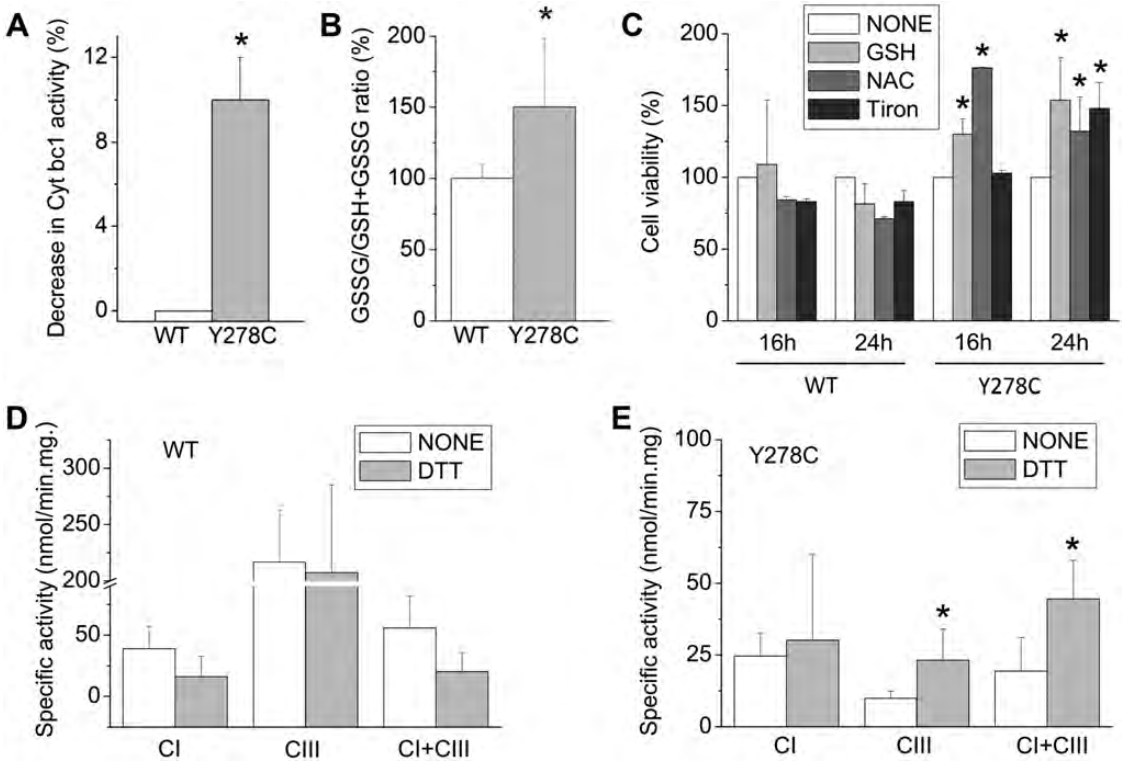

Figure 3. Superoxide production and glutathione homeostasis. (**A**) The rate of superoxide production was determined in isolated mitochondria by the manganese-SOD-induced decrease of DBH_2:cytochrome *c* reduction rates that are sensitive to CIII inhibitor stigmatellin, as described in Materials and Methods. Rates were corrected for stigmatellin-insensitive (i.e. cytochrome bc_1-independent) rates. Data are presented as the means ± SD of three determinations; asterisk denotes the values significantly different from controls ($^*P < 0.05$). (**B**) Cells were incubated in DMEM-galactose for 6 h and the GSSG/GSH + GSSG ratio was measured as described in Materials and Methods. Values are expressed as percent increase over controls. Data are presented as the means ± SD of three determinations, and asterisk denotes the values significantly different from controls ($^*P < 0.05$). (**C**) Cybrids were incubated in DMEM-galactose in the absence or the presence of 10 mM GSH or 10 mM NAC or 10 mM Tiron. The 100% value corresponds to viability determined for each cell line after incubation for the indicated times in DMEM-galactose. Values are presented as the means ± SD of three determinations. Asterisk denotes a value significantly different from untreated cells (none, $^*P < 0.05$). The respiratory complexes activities (CI, CIII and CI + CIII) were determined in crude mitochondria from wild-type (**D**) and mutated (**E**) cybrids isolated in a buffer without or with 10 mM DTT, as described in Materials and Methods. Data are presented as the means ± SD of five determinations. Asterisk denotes the values significantly different from those obtained without DTT ($^*P < 0.05$).

respiratory chain complexes, using blue-native gel electrophoresis (BN-PAGE) in the presence of dodecylmaltoside (DDM), which completely disperses respiratory supercomplexes (25), also did not show any significant difference between control and mutant cells when their ratios to the CII amounts present in each blot were compared (Fig. 4B). Taken together, these results suggest that the mutation affects the CIII activity but not the CIII steady-state levels. We next examined the supramolecular organization of respiratory supercomplexes with BN-PAGE in the presence of high concentration of the mild detergent digitonin, which keeps intact loose interactions between complexes. Interestingly, significant changes associated with CIII identified by the Core2 antibody were observed. Band intensities corresponding to the dimeric CIII and the supercomplex III_2IV_1 were markedly decreased, whereas those corresponding to the supercomplex $I_1III_2IV_n$ increased slightly (Fig. 5Ac and a, respectively). No appreciable difference was observed in the band intensities attributed to the other complexes (CII, CIV and CV, shown in Fig. 5Ab, d and e, see quantification in Supplementary Material, Fig. S3A). These observations were further confirmed by second dimension (2D) BN-PAGE/SDS–PAGE analysis, using antibodies against both Core2 and also the Rieske Fe/S protein of CIII (Fig. 5B, top two lanes). Clearly, the spots corresponding to the CIII dimer and the $CIII_2IV_1$ supercomplex were reduced in Y278C when compared with control cells. In contrast, no remarkable changes were seen in the amounts of the $CI_1III_2IV_n$ supercomplex, as indicated by the anti-Core2, Rieske, NDUFS3 and CoxIV antibodies (semi-quantitative evaluation of band intensities is reported in Supplementary Material, Fig. S3B). Furthermore, CI-associated in-gel activity (IGA), detected in parallel experiments, was slightly increased (Fig. 5C), suggesting that the p.278Y>C mutation does not decrease the CI levels nor impair the complex/supercomplex assembly.

Finally, the measurement of the CIII and CI + CIII activities of digitonin- and DDM-extracted mitoplasts from mutant and control cybrids was carried out, i.e. under conditions favoring or preventing, respectively, the CIII assembly in the supercomplexes. Figure 5D shows that the ratio of the residual CIII activity of the mutant over control was significantly higher in digitonin-treated mitoplasts compared with both crude and DDM-treated mitoplasts, whereas the ratio of the CI + CIII activity was similar in crude and digitonin-

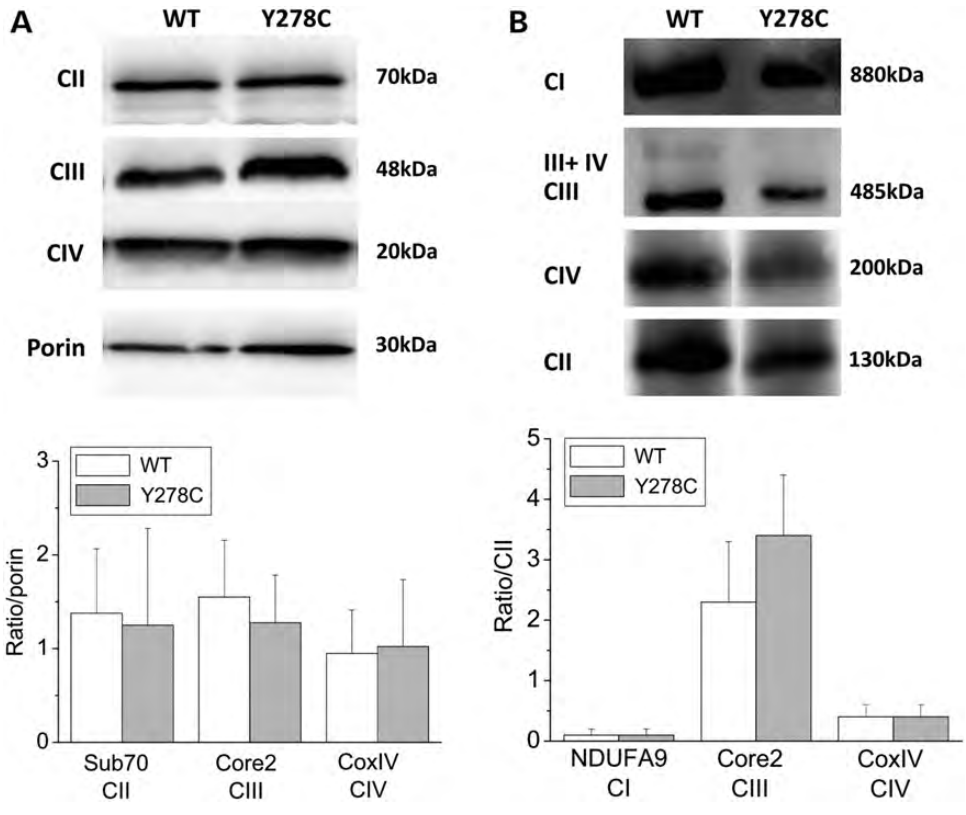

Figure 4. Expression level and assembly of respiratory complexes. (**A**) Respiratory chain subunits from mitoplasts obtained as described in Materials and Methods were separated by SDS–PAGE and western blot analysis carried out using the antibodies against the CII-subunit 70, the CIII-Core 2 and the CIV-COVIX subunits. The signal corresponding to porin was used for normalization. Results are presented as the means ± SD from four independent blots. (**B**) Western blot analysis of the respiratory complexes subunits after BN-PAGE of DDM-solubilized mitoplasts. The antibodies were against the CI-NDUFA9 subunit, the CII-subunit 70 kDa, the CIII-Core 2 and the CIV-COVIX subunit. The intensity of bands was normalized against the CII subunit. Data are presented as the mean ± SD of four blots.

treated mitoplasts. As expected, the CI + CIII activity was completely abolished in DDM-treated mitoplasts. These findings suggest that the organization of respiratory complexes into natural supercomplexes apparently provides beneficial consequences in the case of cytochrome *b* p.278Y>C mutant CIII, which is more readily damaged when present alone in energy transducing membranes.

DISCUSSION

In the present study, we dissect the biochemical alterations caused in cybrids by the p.278Y>C homoplasmic mutation in cytochrome *b*, analyzing the CIII activity, ROS production and supercomplexes assembly/stability. A major finding of this study is that although this mutation decreased dramatically the CIII activity, the overall CI + CIII activity, ATP synthesis driven by the CI and CII substrates and the mitochondrial membrane potential were only weakly affected. Moreover, in contrast to other cytochrome *b* mutations (8,9), the p.278Y>C substitution did not affect the steady-state levels of CIII and preserved the stability and function of CI, confirming the structural dependence between CI and CIII (11).

Another important finding of this study is that the p.278Y>C mutation enhanced superoxide production by CIII. We note that the occurrence of an oxidative damage as a consequence of the p.278Y>C mutation is a novel finding, since this important issue has not been investigated in the original case report describing the clinical features of the patient (16). We show here that this mutation also induced an imbalance in the cellular GSSG/GSSG + GSH ratio, especially when cells were forced to use the oxidative phosphorylation. Consequently, treatments with the specific superoxide scavenger Tiron (26) or with antioxidant compounds like GSH and NAC significantly ameliorated mutant cells viability under these conditions, indicating that these cells were experiencing oxidative damages in addition to energetic defects. In fact, the rapid loss of viability seen with the p.278Y>C cybrids incubated in the galactose medium can be hardly explained by an exclusive energy dysfunction, considering that in these cells neither the ATP synthesis is completely abolished nor the mitochondrial membrane potential is fully collapsed. A more likely possibility is that the severe loss of viability seen in the galactose medium might be due to synergistic effects of energetic impairment and superoxide overproduction altogether. In agreement with this possibility, it is noteworthy that the activities of CIII and CI + CIII complexes increased significantly when mitochondria were isolated from mutant cells in the presence of a reducing agent like DTT. Thus, the use of reducing conditions might diminish oxidative damages and their consequences such as the plausible formation of an

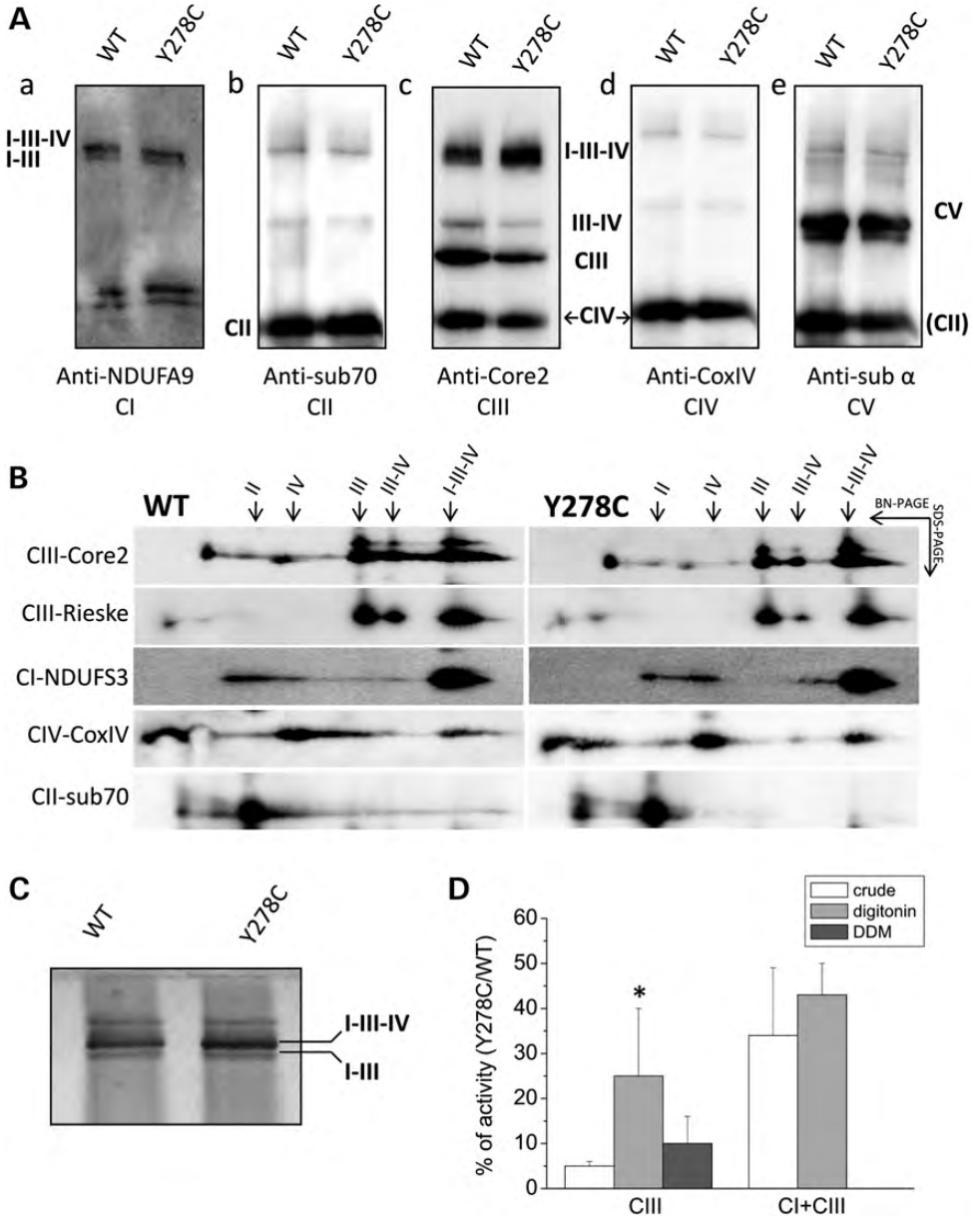

Figure 5. Assembly of oxidative phosphorylation supercomplexes. Analysis of supercomplexes assembly was carried out in digitonin-treated mitoplasts resolved by BN-PAGE, as described in Materials and Methods. Four different gels were loaded for each experiment. (**A**) After electrophoresis, two gels were used for western blotting. The first membrane was incubated with CI-NDUFA9 (a), then with CII-subunit 70 (b) and finally with CV-α-subunit (e) antibodies. The second membrane was first incubated with CIV-COXIV (d) and then with CIII-Core 2 (c) antibodies. The analysis was repeated three times and a representative blot is presented. (**B**) The third gel was used for the separation of strips by second dimension SDS–PAGE. Spots were detected with antibodies against the indicated subunits. A representative blot is shown. (**C**) The last gel obtained from BN-PAGE was processed for the CI IGA, as described in Materials and Methods. (**D**) CIII and CI + CIII activities were determined in crude mitochondria, in mitoplasts solubilized with digitonin and in mitoplasts solubilized with DDM, as detailed in Materials and Methods. Data are expressed as the ratio of mutant to wild-type enzymatic activity. Data are presented as the means ± SD of at least six determinations. Asterisk denotes the values significantly different from those of digitonin-solubilized mitoplasts ($^{*}P < 0.05$).

inter-subunit disulfide bond between the Fe/S protein and cytochrome *b* upon exposure to oxygen, as seen with the bacterial case (17).

The third original finding of our study concerns the altered supramolecular organization of supercomplexes in mutant cybrids. Decreased amounts of CIII dimer and supercomplex III_2IV_1 seen in the mutant case may reflect the reduced stability or enhanced degradation of these complexes, implying that mutated CIII is better protected by oxygen when included within the $I_1III_2IV_n$ supercomplex. Our prevailing hypothesis is that in mutated cybrids, the reduced activity of CIII carrying the p.278Y>C mutation is essentially due to the malfunction and decreased amount of the $CIII_2$ and $CIII_2IV_1$ as a consequence of their oxygen liability. A direct support for this proposal stems from the observation that the ratio of the residual CIII activity in mutated and control cells is higher in digitonin-

solubilized mitoplasts. This treatment preserves better the supercomplex organization, hence protects indirectly CIII, from damaging effects of O_2. In contrast, crude mitochondria are likely to be more exposed to O_2 during the isolation procedure, and in DDM-solubilized mitoplasts, the supercomplexes are completely dispersed. The low residual CIII activity ratio observed in crude mitochondria, where a significant fraction of CIII should be present in the $I_1III_2IV_n$ supercomplex, is likely due to oxidative damages given that the mutant CIII activity was significantly increased when mitochondria were isolated in the presence of DTT. Finally, it is noteworthy that the mutant to wild-type ratio of CI + CIII activities is similar in both crude and digitonized mitoplasts, suggesting that a fraction of CIII is still functioning in supercomplex $I_1III_2IV_n$ and is protected from O_2. Indeed, a more direct comparison of the activity of CIII associated within the $I_1III_2IV_n$ supercomplex with that of dimeric CIII would better document our hypothesis. Unfortunately, we were unable to obtain reliable data using spectrophotometric determination of the CIII activity after extraction/homogenization of bands from native gels using mitochondria from cultured cells. At present, the only staining method described for the CIII IGA has been shown to work only in mitochondria from the human skeletal muscle and liver (27).

In conclusion, the findings of this study have important implications on the functional significance of supercomplexes, revealing their usefulness not only for channeling electron transport between complexes, but also for mitigating the detrimental effects of pathogenic mutations. It is well known that deleterious mtDNA mutations are often found in some but not all of the mitochondrial genomes and that the ratio of wild-type to mutant mtDNA determines the onset of clinical symptoms. The minimum critical proportion of mutated mtDNA required to exhibit the biochemical defects is defined as the 'threshold effect' (28). Typically, the threshold value is in the range of 60–90% mutant to wild-type mtDNA depending on the mutation type and is different among the tissues. Although the threshold level can partly explain the disease phenotypes observed in patients, an exact correlation between clinical severity and the proportion of mtDNA mutation is often unclear, suggesting that other factors also contribute to the functional achievement of such threshold (29). The results stemming from the p.278Y>C mutant cybrids point out that these cells are still able to maintain partially their oxidative phosphorylation capability despite the strong deficiency in the CIII activity. Thus, at least in this instance, supercomplexes seem to modulate the overall efficiency of oxidative phosphorylation. Moreover, ROS production deriving from an altered CIII may contribute to a chronic oxidative stress as a relevant modifying factor for the onset and progression of the disease.

We believe that the detailed characterization of the effects of single cytochrome *b* mutations might yield exclusive clues for therapeutic interventions. For example, our findings suggest that treatments with superoxide scavengers or antioxidants or with chemicals enhancing supercomplex formation may be envisaged as possible strategies to palliate multisystemic symptoms associated with the p.278Y>C and similar mutations. The catalytic subunits of CIII being evolutionarily well conserved, detailed comparative analyses of the biochemical alterations induced by cytochrome *b* mutations conducted in parallel using complementary cellular and bacterial models might be beneficial. They will allow the use of sophisticated biochemical methods that require large amounts of purified membranes or enzymes, such as EPR spectroscopy or X-ray crystallography, respectively, for assessing therapeutic options toward innovative strategies for treatments of CIII-related mitochondrial diseases.

MATERIALS AND METHODS

Materials

ATP, DCIP, 2,3-dimethoxy-5-methyl-6-decyl-1,4-benzoquinone (DB), NADH, cytochrome *c*, malate, pyruvate, succinate, antimycin A, stigmatellin, malonate, oligomycin, rotenone, P^1,P^5-di(adenosine-5′) pentaphosphate pentasodium salt, carbonyl cyanide 4-(trifluoromethoxy) phenylhydrazone (FCCP), sulforhodamine B (SRB), DTT, digitonin, DDM, GSH and GSSG, NAC, Tiron and the ATP monitoring kit were purchased from Sigma-Aldrich (Milan, Italy). TMRM methyl ester was from Molecular Probes (Eugene, OR, USA). The antibodies against porin (BioVision, Mountain View, CA, USA), NDUFA9 and NDUFS3 (CI), subunit 70 kDa (CII), Core2 and Rieske (CIII), subunit IV (CIV) and subunit α (CV) were from MitoSciences (Eugene, OR, USA). Secondary antibodies were from Jackson ImmunoResearch Europe Ltd (Soham, Cambridgeshire, UK).

Cell lines and culture conditions

Cybrid cell lines were generated using enucleated fibroblasts bearing the m.15579A>G (p.278Y>C) cytochrome *b* mutation (16) as mitochondria donors, and the mtDNA-deprived human osteosarcoma 143B.TK$^-$ cell line (Rho0 cells) as the acceptor, following the protocols described elsewhere (30). Cybrids were grown in DMEM supplemented with 10% fetal calf serum (South America source from Gibco, Invitrogen, Italy), 2 mM L-glutamine, 100 U/ml penicillin and 100 μg/ml streptomycin, in an incubator with a humidified atmosphere of 5% CO_2 at 37°C. In some experiments, cells were incubated with a glucose-free DMEM supplemented with 5 mM galactose, 5 mM sodium pyruvate and 5% fetal calf serum (DMEM-galactose).

MtDNA analysis

The homoplasmic/heteroplasmic state of the cybrid cell clones was defined by PCR/restriction fragment length polymorphism. Restriction fragments were separated by electrophoresis on the Metaphor (BioSpa) gel at 4% and detected by ethidium bromide staining. Densitometric analysis was performed using AlphaView software package (Cell Biosciences). Primers, PCR and restriction endonuclease reaction conditions are available upon request.

MtDNA sequence analysis was carried out as described previously (31). The mutant load of the m.15579A>G mutation was determined by DHPLC by comparison of mutant clones to a standard curve ($y = 174.1x - 184.2$; $R^2 = 0.992$) (18). Briefly, DNA was extracted using GeneElute Mammalian

Genomic DNA Miniprep Kit (Sigma-Aldrich) and amplified, together with artificial heteroplasmy standards, using 5′-ACGAAACGGGATCAAACAAC-3′ and 5′-GGAGGAT GGGGATTATTGCT-3′ primers (18). The PCR products were denaturated for 10 min at 95°C and analyzed with WAVE Nucleic Acid Fragment Analysis System (Transgenomic, Omaha, NE, USA), applying 58.7°C as the optimal separation temperature. The primers were designed following the criteria for exclusion of nuclear mitochondrial sequences co-amplification and artificial heteroplasmy standards were prepared as described previously (18).

Cell viability

Cybrid clones were seeded (4×10^4 cells/cm^2) in 24-well plates and incubated with DMEM or with DMEM-galactose. At the times indicated, cell viability was measured by the SRB absorbance at 570 nm with a VICTOR3 Multilabel Plate Counter (PerkinElmer Life and Analytical Sciences, Zaventem, Belgium) (32).

Subcellular fractionation

Crude mitochondria were obtained by harvesting $\sim 15 \times 10^6$ cells in phosphate-buffered saline (PBS). After centrifugation, the pellet was suspended in the isolation buffer containing 0.25 M sucrose, 10 mM Tris–Cl, pH 7.5, and 0.1 mM phenylmethylsulfonyl fluoride (PMSF) and homogenized using a glass Teflon homogenizer. This and all the subsequent procedures were carried out at 4°C. When indicated, 10 mM DTT was added to the isolation buffer. Unbroken cells and nuclei were centrifuged at 600*g* for 20 min, and the supernatant was centrifuged again at 10 000*g* for 20 min. The mitochondrial pellet was suspended with the isolation buffer and stored at −80°C, after determination of the protein content (33).

Mitoplasts were isolated from cell pellets ($\sim 10 \times 10^6$ cells) using digitonin (final concentration of 50 μg/ml) (34). For supercomplex analysis, mitoplasts were suspended in PBS and protein concentration was determined (33). After centrifugation, the pellet was suspended (final concentration 5 mg protein/ml) in 150 mM K-acetate, 30 mM 4-(2-hydroxyethyl)-1-piperazineethanesulfonic acid (HEPES), pH 7.4, 10% glycerol, 1 mM PMSF, 10 mg/ml digitonin and incubated on ice for 30 min (34). Samples were centrifuged for 2 min at 600*g* and supernatant was used for the spectrophotometric assay or BN-PAGE (see below).

To analyze isolated native complexes, mitoplasts were suspended in a buffer containing 750 mM aminocaproic acid, 50 mM bis–tris, pH 7.0, and solubilized with DDM (20%), corresponding to a DDM/protein ratio of 2.5 (g/g). The suspension was incubated on ice for 10 min and then centrifuged at 13 000*g* for 15 min (34). The supernatant was used for the spectrophotometric assay or BN-PAGE (see below). In a set of experiments, the same mitoplasts preparation was split into two aliquots that were processed in parallel to obtain supercomplexes (digitonized-mitoplasts) and isolated native complexes (DDM-mitoplasts).

Respiratory complex activity

Crude mitochondria, mitoplasts treated for supercomplexes (digitonized) or for native complexes (DDM-solubilized) analysis, as described above, obtained from wild-type and mutant cybrids grown in DMEM were incubated in a buffer containing 50 mM potassium phosphate, pH 7.8, 0.35% bovine serum albumin and 0.3 mM KCN. The redox enzymatic activities were measured at 37°C by using a dual-wavelength spectrophotometer (V550 Jasco Europe, Italy). The CI activity (NADH:DB:DCIP oxidoreductase) was assessed in the presence of 60 μM DCIP (λ: 600 nm; ϵ_{DCIP}: 19.1/mM/cm), 70 μM DB and 200 μM NADH, as described previously (23), after the subtraction of 1 μM rotenone-insensitive activity. The CI + CIII activity (NADH:cytochrome *c* reductase) was performed in the presence 200 μM NADH and 20 μM bovine heart cytochrome *c* (λ: 550–540 nm; $\epsilon_{cytc} = 19.1$/mM/cm), after the subtraction of 1 μM rotenone- and 1 μM antimycin A-insensitive activity. The CIII activity was determined as the antimycin A-sensitive ubiquinol:cytochrome *c* reductase activity in the presence of 50 μM decylbenzoquinol (DBH_2) reduced as described in Rieske (35) and 20 μM bovine heart cytochrome *c*, as described previously (36). The CII + CIII activity was measured as the succinate:cytochrome *c* reductase activity in the presence of 5 mM succinate and 20 μM bovine heart cytochrome *c*, after the subtraction of 5 mM malonate- and 1 μM antimycin A-insensitive activity.

Mitochondrial ATP synthesis

The rate of mitochondrial ATP synthesis was measured in digitonin-permeabilized control and mutant cybrids by using the luciferin/luciferase assay, according to the methods described previously (37), with minor modifications (38). Briefly, after trypsinization, cells (10×10^6/ml) were suspended in a buffer containing 150 mM KCl, 25 mM Tris–HCl, 2 mM EDTA (ethylenediaminetetraacetic acid), 0.1% bovine serum albumin, 10 mM potassium phosphate, 0.1 mM $MgCl_2$, pH 7.4, kept at room temperature for 15 min, then incubated with 50 μg/ml digitonin until 90–100% of cells were positive to Trypan blue staining. Aliquots of 3×10^5 permeabilized cells were incubated in the same buffer in the presence of the adenylate kinase inhibitor P^1,P^5-di(adenosine-5′) pentaphosphate (0.1 mM) and the CI substrates (5 mM malate plus 5 mM pyruvate) or the CII substrate (10 mM succinate plus 2 μg/ml rotenone) or the CIII substrate (50 μM DBH_2 plus 1 μM rotenone and 5 mM malonate). After the addition of 0.2 mM ADP, chemiluminescence was determined as a function of time with a luminometer. The chemiluminescence signal was calibrated with an internal ATP standard after the addition of 10 μM oligomycin. The rates of the ATP synthesis were normalized to protein contents (33) and the citrate synthase (CS) activity (22).

Mitochondrial membrane potential ($\Delta\psi_m$)

Cells were seeded onto 24 mm diameter round glass coverslips and grown for 2 days in DMEM. $\Delta\psi_m$ was measured by the accumulation of TMRM, as described in Porcelli *et al*. (39). Briefly, cells were incubated in Hank's balanced salt solution

containing 10 mM HEPES (Sigma-Aldrich) and 20 nM TMRM for 30 min and fluorescence images were acquired with a Nikon Ti-U inverted microscope, equipped with a back-illuminated Photometrics Cascade CCD camera system (Roper Scientific, Tucson, AZ, USA) and Metafluor acquisition/analysis software (Universal Imaging Corp., Downingtown, PA, USA). Clusters of several mitochondria (8–12) were identified as the regions of interest, and fields not containing cells were taken as the background. Sequential digital images and fluorescence intensities were acquired every minute. At each time-point, fluorescence values were obtained after the subtraction of the background values from those of the corresponding mitochondrial regions of interest. Data are expressed as percentage of the initial fluorescence value (measured at time = 0).

Superoxide measurement and determination of the GSH/GSSG content

The rate of superoxide production by mitochondria isolated from wild-type and mutant cybrids was determined using manganese-SOD- and stigmatellin-sensitive cytochrome *c* reduction in the presence of 50 μM DBH_2, as described previously (17). The GSH and GSSG contents of cybrids incubated in DMEM and DMEM-galactose were determined enzymatically, as described in Ghelli *et al*. (40). Values were expressed as the percent increase over wild-type cells.

Sodium dodecyl sulfate–polyacrylamide gel electrophoresis

Mitoplasts were solubilized in radio-immunoprecipitation assay buffer and the protein content was measured (33). About 40 μg of proteins were separated by 12% SDS–PAGE and transferred onto a nitrocellulose membrane (Bio-Rad, Hertfordshire, UK) for western blotting analysis.

Analysis of native complex assembly

To isolated native complexes (100 μg), prepared as described above, sample buffer (5% Serva G Blue in 750 mM aminocaproic acid, 50 mM bis–tris and 0.5 mM EDTA) was added before loading on the 4–12% gradient gel. Samples were loaded in duplicated on clear native-PAGE (CN-PAGE) and BN-PAGE as described in Wittig *et al*. (34). After electrophoresis, the samples on the CN-PAGE gel were processed for CI IGA as described in Porcelli *et al*. (39) and the samples on the BN-PAGE gel were used for western blotting.

Analysis of supercomplex assembly and 2D BN-PAGE/SDS–PAGE

Mitoplasts treated for supercomplexes analysis, as described above, were separated on the 3–12% gradient gel (BN-PAGE) (11). Briefly, 100 μg of samples was loaded on the gel after the addition of 5% Serva G Blue in 750 mM aminocaproic acid. After electrophoresis, gels were processed for IGA (39), western blotting or second dimension SDS–PAGE (2D BN-PAGE/SDS–PAGE). Strips from the first dimension 3–12% gradient gel were excised and then used for 2D BN-PAGE/SDS–PAGE. Each strip was treated with denaturing buffer containing 1% SDS and 0.1% β-mercaptoethanol for 90 min and then separated on 10% SDS–PAGE as described in Calvaruso *et al*. (41). After electrophoresis, gels were used for western blotting.

Western blotting

Gels were transferred on nitrocellulose membrane (Bio-Rad) for 1 h at 100 V. The nitrocellulose membranes were incubated overnight at 4°C with anti-NDUFA9 CI (1:1000), anti-70 kDa subunit CII (1:10 000), anti-αATPase CV (1:1000), anti-COXIV CIV (1:1000), anti-CORE2 CIII (1:1000) and anti-NDUFS3 CI (1:1000). Primary antibodies were visualized using horseradish peroxidase-conjugated secondary antibodies (1:2000). The chemiluminescence signals were revealed using an ECL western blotting kit (Amersham Bioscience, Buckinghamshire, UK) and measured with Gel Logic 1500 Imaging System, Kodak.

Statistics

All experiments were repeated at least three times, and the results are presented as the mean ± SD, unless otherwise indicated. Statistical analysis was performed using the Student's *t*-test, with $P < 0.05$ as the level of significance.

SUPPLEMENTARY MATERIAL

Supplementary Material is available at *HMG* online.

ACKNOWLEDGEMENTS

We thank Dr Valerio Carelli and Dr Marialuisa Genova, University of Bologna, for helpful discussion and critically reading the manuscript.

Conflict of Interest statement. None declared.

FUNDING

This work was supported by National Institutes of Health (GM 38237 to F.D. and M.R.), providing fellowships to A.M. and C.V.T., and partially by the ERMION grant to M.R. and a grant FIRB 'Futuro in Ricerca' (Ministero dell'Istruzione, dell'Università e della Ricerca) to G.G.

REFERENCES

1. Berry, E.A., Guergova-Kuras, M., Huang, L.S. and Crofts, A.R. (2000) Structure and function of cytochrome bc complexes. *Annu. Rev. Biochem.*, **69**, 1005–1075.
2. Osyczka, A., Moser, C.C., Daldal, F. and Dutton, P.L. (2004) Reversible redox energy coupling in electron transfer chains. *Nature*, **427**, 607–612.
3. Schagger, H. and Pfeiffer, K. (2000) Supercomplexes in the respiratory chains of yeast and mammalian mitochondria. *EMBO J.*, **19**, 1777–1783.
4. Althoff, T., Mills, D.J., Popot, J.L. and Kuhlbrandt, W. (2011) Arrangement of electron transport chain components in bovine mitochondrial supercomplex I(1)III(2)IV(1). *EMBO J.*, **30**, 4652–4664.
5. Schafer, E., Dencher, N.A., Vonck, J. and Parcej, D.N. (2007) Three-dimensional structure of the respiratory chain supercomplex

I1III2IV1 from bovine heart mitochondria. *Biochemistry*, **46**, 12579–12585.
6. Acin-Perez, R., Fernandez-Silva, P., Peleato, M.L., Perez-Martos, A. and Enriquez, J.A. (2008) Respiratory active mitochondrial supercomplexes. *Mol. Cell*, **32**, 529–539.
7. Lenaz, G. and Genova, M.L. (2010) Structure and organization of mitochondrial respiratory complexes: a new understanding of an old subject. *Antioxid. Redox Signal.*, **12**, 961–1008.
8. Acin-Perez, R., Bayona-Bafaluy, M.P., Fernandez-Silva, P., Moreno-Loshuertos, R., Perez-Martos, A., Bruno, C., Moraes, C.T. and Enriquez, J.A. (2004) Respiratory complex III is required to maintain complex I in mammalian mitochondria. *Mol. Cell*, **13**, 805–815.
9. Blakely, E.L., Mitchell, A.L., Fisher, N., Meunier, B., Nijtmans, L.G., Schaefer, A.M., Jackson, M.J., Turnbull, D.M. and Taylor, R.W. (2005) A mitochondrial cytochrome b mutation causing severe respiratory chain enzyme deficiency in humans and yeast. *FEBS J.*, **272**, 3583–3592.
10. Budde, S.M., van den Heuvel, L.P., Janssen, A.J., Smeets, R.J., Buskens, C.A., DeMeirleir, L., Van Coster, R., Baethmann, M., Voit, T., Trijbels, J.M. *et al.* (2000) Combined enzymatic complex I and III deficiency associated with mutations in the nuclear encoded NDUFS4 gene. *Biochem. Biophys. Res. Commun.*, **275**, 63–68.
11. Calvaruso, M.A., Willems, P., van den Brand, M., Valsecchi, F., Kruse, S., Palmiter, R., Smeitink, J. and Nijtmans, L. (2011) Mitochondrial complex III stabilizes complex I in the absence of NDUFS4 to provide partial activity. *Hum. Mol. Genet.*, **21**, 115–120.
12. Benit, P., Lebon, S. and Rustin, P. (2009) Respiratory-chain diseases related to complex III deficiency. *Biochim. Biophys. Acta*, **1793**, 181–185.
13. Andreu, A.L., Hanna, M.G., Reichmann, H., Bruno, C., Penn, A.S., Tanji, K., Pallotti, F., Iwata, S., Bonilla, E., Lach, B. *et al.* (1999) Exercise intolerance due to mutations in the cytochrome b gene of mitochondrial DNA. *N. Engl. J. Med.*, **341**, 1037–1044.
14. Keightley, J.A., Anitori, R., Burton, M.D., Quan, F., Buist, N.R. and Kennaway, N.G. (2000) Mitochondrial encephalomyopathy and complex III deficiency associated with a stop-codon mutation in the cytochrome b gene. *Am. J. Hum. Genet.*, **67**, 1400–1410.
15. Rana, M., de Coo, I., Diaz, F., Smeets, H. and Moraes, C.T. (2000) An out-of-frame cytochrome b gene deletion from a patient with parkinsonism is associated with impaired complex III assembly and an increase in free radical production. *Ann. Neurol.*, **48**, 774–781.
16. Wibrand, F., Ravn, K., Schwartz, M., Rosenberg, T., Horn, N. and Vissing, J. (2001) Multisystem disorder associated with a missense mutation in the mitochondrial cytochrome b gene. *Ann. Neurol.*, **50**, 540–543.
17. Lee, D.W., Selamoglu, N., Lanciano, P., Cooley, J.W., Forquer, I., Kramer, D.M. and Daldal, F. (2011) Loss of a conserved tyrosine residue of cytochrome b induces reactive oxygen species production by cytochrome bc1. *J. Biol. Chem.*, **286**, 18139–18148.
18. Kurelac, I., Lang, M., Zuntini, R., Calabrese, C., Simone, D., Vicario, S., Santamaria, M., Attimonelli, M., Romeo, G. and Gasparre, G. (2010) Searching for a needle in the haystack: comparing six methods to evaluate heteroplasmy in difficult sequence context. *Biotechnol. Adv.*, **30**, 363–671.
19. Robinson, B.H. (1996) Use of fibroblast and lymphoblast cultures for detection of respiratory chain defects. *Methods Enzymol.*, **264**, 454–464.
20. Ghelli, A., Zanna, C., Porcelli, A.M., Schapira, A.H., Martinuzzi, A., Carelli, V. and Rugolo, M. (2003) Leber's hereditary optic neuropathy (LHON) pathogenic mutations induce mitochondrial-dependent apoptotic death in transmitochondrial cells incubated with galactose medium. *J. Biol. Chem.*, **278**, 4145–4150.
21. D'Aurelio, M., Gajewski, C.D., Lenaz, G. and Manfredi, G. (2006) Respiratory chain supercomplexes set the threshold for respiration defects in human mtDNA mutant cybrids. *Hum. Mol. Genet.*, **15**, 2157–2169.
22. Trounce, I.A., Kim, Y.L., Jun, A.S. and Wallace, D.C. (1996) Assessment of mitochondrial oxidative phosphorylation in patient muscle biopsies, lymphoblasts, and transmitochondrial cell lines. *Methods Enzymol.*, **264**, 484–509.
23. Janssen, A.J., Trijbels, F.J., Sengers, R.C., Smeitink, J.A., van den Heuvel, L.P., Wintjes, L.T., Stoltenborg-Hogenkamp, B.J. and Rodenburg, R.J. (2007) Spectrophotometric assay for complex I of the respiratory chain in tissue samples and cultured fibroblasts. *Clin. Chem.*, **53**, 729–734.
24. Hansen, J.M., Go, Y.M. and Jones, D.P. (2006) Nuclear and mitochondrial compartmentation of oxidative stress and redox signaling. *Annu. Rev. Pharmacol. Toxicol.*, **46**, 215–234.
25. Nijtmans, L.G., Henderson, N.S. and Holt, I.J. (2002) Blue Native electrophoresis to study mitochondrial and other protein complexes. *Methods*, **26**, 327–334.
26. Taiwo, F.A. (2008) Mechanism of tiron as scavanger of superoxide ions and free electrons. *Spectroscopy*, **22**, 491–498.
27. Smet, J., De Paepe, B., Seneca, S., Lissens, W., Kotarsky, H., De Meirleir, L., Fellman, V. and Van Coster, R. (2011) Complex III staining in blue native polyacrylamide gels. *J. Inherit. Metab. Dis.*, **34**, 741–747.
28. DiMauro, S. and Schon, E.A. (2008) Mitochondrial disorders in the nervous system. *Annu. Rev. Neurosci.*, **31**, 91–123.
29. Tuppen, H.A., Blakely, E.L., Turnbull, D.M. and Taylor, R.W. (2009) Mitochondrial DNA mutations and human disease. *Biochim. Biophys. Acta*, **1797**, 113–128.
30. King, M.P. and Attardi, G. (1996) Isolation of human cell lines lacking mitochondrial DNA. *Methods Enzymol.*, **264**, 304–313.
31. Bonora, E., Porcelli, A.M., Gasparre, G., Biondi, A., Ghelli, A., Carelli, V., Baracca, A., Tallini, G., Martinuzzi, A., Lenaz, G. *et al.* (2006) Defective oxidative phosphorylation in thyroid oncocytic carcinoma is associated with pathogenic mitochondrial DNA mutations affecting complexes I and III. *Cancer Res.*, **66**, 6087–6096.
32. Porcelli, A.M., Ghelli, A., Iommarini, L., Mariani, E., Hoque, M., Zanna, C., Gasparre, G. and Rugolo, M. (2008) The antioxidant function of Bcl-2 preserves cytoskeletal stability of cells with defective respiratory complex I. *Cell. Mol. Life Sci.*, **65**, 2943–2951.
33. Bradford, M.M. (1976) A rapid and sensitive method for the quantitation of microgram quantities of protein utilizing the principle of protein-dye binding. *Anal. Biochem.*, **72**, 248–254.
34. Wittig, I., Karas, M. and Schagger, H. (2007) High resolution clear native electrophoresis for in-gel functional assays and fluorescence studies of membrane protein complexes. *Mol. Cell. Proteomics*, **6**, 1215–1225.
35. Rieske, J. (1967) Preparation and properties of reduced coenzyme Q-cytochrome Q oxidoreductase of the mitochondrial respiratory chain. *Methods Enzymol.*, **X**, 239–245.
36. Fato, R., Cavazzoni, M., Castelluccio, C., Parenti Castelli, G., Palmer, G., Degli Esposti, M. and Lenaz, G. (1993) Steady-state kinetics of ubiquinol-cytochrome c reductase in bovine heart submitochondrial particles: diffusional effects. *Biochem. J.*, **290**, 225–236.
37. Manfredi, G., Yang, L., Gajewski, C.D. and Mattiazzi, M. (2002) Measurements of ATP in mammalian cells. *Methods*, **26**, 317–326.
38. Giorgio, V., Petronilli, V., Ghelli, A., Carelli, V., Rugolo, M., Lenaz, G. and Bernardi, P. (2012) The effects of idebenone on mitochondrial bioenergetics. *Biochim. Biophys. Acta*, **1817**, 363–369.
39. Porcelli, A.M., Angelin, A., Ghelli, A., Mariani, E., Martinuzzi, A., Carelli, V., Petronilli, V., Bernardi, P. and Rugolo, M. (2009) Respiratory complex I dysfunction due to mitochondrial DNA mutations shifts the voltage threshold for opening of the permeability transition pore toward resting levels. *J. Biol. Chem.*, **284**, 2045–2052.
40. Ghelli, A., Porcelli, A.M., Zanna, C., Martinuzzi, A., Carelli, V. and Rugolo, M. (2008) Protection against oxidant-induced apoptosis by exogenous glutathione in Leber hereditary optic neuropathy cybrids. *Invest. Ophthalmol. Vis. Sci.*, **49**, 671–676.
41. Calvaruso, M.A., Smeitink, J. and Nijtmans, L. (2008) Electrophoresis techniques to investigate defects in oxidative phosphorylation. *Methods*, **46**, 281–287.